Available online at www.sciencedirect.com

ScienceDirect

Procedia Manufacturing 25 (2018) 322–329

Procedia MANUFACTURING

www.elsevier.com/locate/procedia

8th Swedish Production Symposium, SPS 2018, 16-18 May 2018, Stockholm, Sweden

Superhard pcBN materials with chromium compounds as a binder

Kateryna Slipchenko[a,b], Vladimir Turkevich[a], Igor Petrusha[a],

Volodymyr Bushlya[b], Jan-Eric Ståhl[b]

[a]*V.N. Bakul Institute for Superhard Materials of NAS of Ukraine, Kyiv 04074, Ukraine*
[b]*Lund University, Division of Production and Materials Engineering, Lund 22100, Sweden*

Abstract

Superhard cBN-based materials with Cr_3C_2, Cr_2N and CrB_2 binders were sintered in a high-pressure high-temperature (HPHT) toroidal apparatus under a pressure of 7.7 GPa and in the temperature range of 1600-2450°C. Initial mixtures of three compositions were chosen with 60 vol.% of cBN, 35 vol.% of binder phase and 5 vol.% of Al. Phase composition and microstructure of sintered samples were investigated by X-ray analysis and scanning electron microscopy, respectively. Elastic properties were measured using the ultrasonic pulse-echo technique. Composites with Cr_3C_2 and CrB_2 binders sintered at 2000°C have the highest values of hardness.

Peer-review under responsibility of the scientific committee of the 8th Swedish Production Symposium.

Keywords: boron nitride, high pressure, cromium carbide, sintering

1. Introduction

Cubic boron nitride (cBN) based composites are widely used for cutting of superalloys and hardened steels due to their good thermal conductivity and high oxidation resistance. Sintering of pure cBN is complicated even under high-pressure high-temperature (HPHT) conditions [1]. Therefore, to assist sintering and improve properties of the composites, additional binder materials are introduced. Binders are classified in two groups: metallic and ceramic.

Powders of high purity metals (Ni, Co, Cr, Fe) are used as a metallic bonding media [2]. Alternatively, Ti and Al are used for reaction sintering with cBN [3-5]. During sintering in the cBN-Ti system, titanium reacts with BN matrix forming TiN and TiB_2. The TiN and TiB_2 phases are uniformly distributed in cBN intergrain space [6-8]. The hardness of this composite without heat treatment is higher than in elemental Ti [9].

2351-9789
Peer-review under responsibility of the scientific committee of the 8th Swedish Production Symposium.
10.1016/j.promfg.2018.06.090

The same tendency exists in the systems sintered with aluminum. Molten Al reacts with cBN to form residual binder phases AlB_2 and AlN. Presence of aluminum compounds increases the thermal stability of final materials. In addition, at high sintering temperature, aluminum can react with residual oxygen from the micropores and form Al_2O_3 [10]. In the past few years many researches were conducted to clarify the properties of cBN-based materials with elements from IV-VI groups of the Periodic table, mostly with Ti compounds [11-13]. Zhang et al. reported on the formation of residual phases in the cBN-HfC-Al system during sintering under a high static pressure of 5 GPa. At 700°C cBN reacted with components of the mixture and produced AlN, AlB_2, HfB_2 and $B_2C_5N_2$. The highest value of hardness 25 GPa was obtained in the system with 70 vol.% of cBN at 1500°C [14]. The authors reported on the formation of $Cr_{6.2}C_{3.5}N_{0.3}$ during HPHT sintering of cBN-Cr_3C_2 (90 vol.% of cBN) [15]. The highest hardness and fracture toughness of cBN-Cr_3C_2 (50 vol.% of cBN) were 22 GPa and 9.7 MPa·$m^{1/2}$, respectively. Materials with low cBN content (45 – 65 vol.%) demonstrated longer tool life during performance testing on Inconel 718 [16]. Ultrahard cNB grains have the greatest influence on the hardness of the final product. In accordance with the approximated Hall-Petch equation [17], the hardness of the composites is inversely proportional to the square root of the grain size. That is why ultrafine cBN powders and Cr_3C_2, Cr_2N, CrB_2 compounds as binder materials were used in this study.

2. Experimental procedure

2.1. Preparation of mixtures

The starting materials used for this work were crushed cBN powders of grades 1-2 and M2-4 (Element Six), Cr_3C_2 (ABCR), Cr_2N (Onyxmet), Cr_2B (Oxynmet) and aluminum flakes (99.7% metals basis, APS 11 μm, produced by ABCR). Particle size distribution analysis (using Malvern Mastersizer 2000 particle size analyser) and XRD analysis were carried out for initial binder materials. Average particle sizes were 1.6 μm for Cr_3C_2, 4 μm for Cr_2N and 6-7 μm for Cr_2B. Chromium nitride and chromium boride binders require milling. Milling of powders was conducted in a Fritsch planetary mill (Pulverisette 6 classic line) equipped with hard tungsten carbide bowl and balls (Ø5-6 mm). Wet milling was carried out for 8 hours at a rate of 200-250 rpm in isopropyl alcohol. Average particle sizes after milling were 2.0 μm for Cr_2N and 1.8 μm for CrB_2. XRD analysis was used to evaluate the traces of milling bodies. For mixture preparation the following ratio was chosen: cBN : binder phase : Al = 60 : 35 : 5 vol.%

Mixtures were homogenized in a gravitational mixer for 3 hours and at 120 rpm. Isopropyl alcohol was used as a mixing medium. After mixing, the mixtures were dried for 8 hours and re-sieved through a sieve.

2.2. Samples sintering

Dried mixtures were placed in the graphite heater and covered by a graphite disk for vacuum annealing (blue lines on Figure 1). Vacuum annealing of the green body was carried out in an SShVL vacuum furnace. The vacuum reached 10^{-5} atm, annealing temperature was 600°C and duration 2 hours. Next the heat-treated green bodies were inserted in high-pressure cells (Figure 1). Sintering was conducted in a toroidal high-pressure apparatus HPA-TOR30 [18] under a pressure of 7.7 GPa. Sintering temperatures were selected in the range of 1600-2450°C with a step of 150°C. The duration of the heating cycle was 45 s, then the power in the circuit was slowly decreased and the pressure released. The obtained samples were ground to RNGN090300T cutting insert shape.

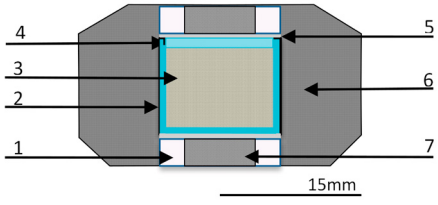

Figure 1. Schematic view of HP-cell for sintering cBN-based materials in HPA TOR30: 1 – pyrophyllite ring; 2 – graphite heater; 3 – mixtures for sintering; 4 – graphite disk; 5 - molybdenum disk; 6 – limestone container; 7 – current lead (graphite + ZrO_2).

2.3. Samples characterization

Phase composition of the sintered samples was determined using a STOE STADI MP X-ray diffractometer (XRD) in Cu Kα radiation. Prior to microscopy and indentation studies the samples were polished with diamond suspension (9 μm and 1 μm) and silica colloidal solution (0.04 μm) using a Struers Tegramin. LEO 1560 scanning electron microscope (SEM) was used for microstructure analysis. Olympus 38D Plus was used for ultrasonic measurements of elastic moduli. Microhardness and fracture toughness were determined using a THV-30MDX Vickers hardness tester. The load on the indenter was 1 kg for measuring hardness and 5 kg for fracture toughness, the dwell time was 15 s. Alicona InfiniteFocus was used for measurements of indentation imprints.

Round RNGN090300T inserts were placed on CRSNL3225P09 toolholder. Cutting conditions corresponded to a finishing operation where feed rate and depth of cut were kept constant $f = 0.15$ mm/rev and $a_p = 0.3$ mm. Longitudinal turning tests were conducted on Torshalla CNC lathe. Two workpiece materials were chosen for the tool life testing: austenitic stainless steel AISI 316L and hardened hot work tool steel Vanadis 4E (HRC 60). Two cutting speeds were employed for machining 316L: $v_c = 500$ m/min and $v_c = 300$ m/min. When hard machining Vanadis 4E, the following cutting speeds were used: $v_c = 200$ m/min and $v_c = 150$ m/min. All tests were conducted with 8% synthetic oil-based emulsion coolant. Machining tests for Vanadis 4E were conducted for a fixed tool engagement length of 600 m, while AISI 316L tests were done for a fixed machining time of 30 sec. Afterwards, the tools wear was measured on Olympus SZX7 stereo microscope.

3. Results and discussion

3.1. Phase composition

Figure 2a shows the XRD patterns of the samples of cBN-Cr_3C_2-Al system sintered under 7.7 GPa at different temperatures. The initial powder mixture consists of cBN and Cr_3C_2 (tongbait), small quantity of aluminium introduced to the mixture is not detected by XRD.

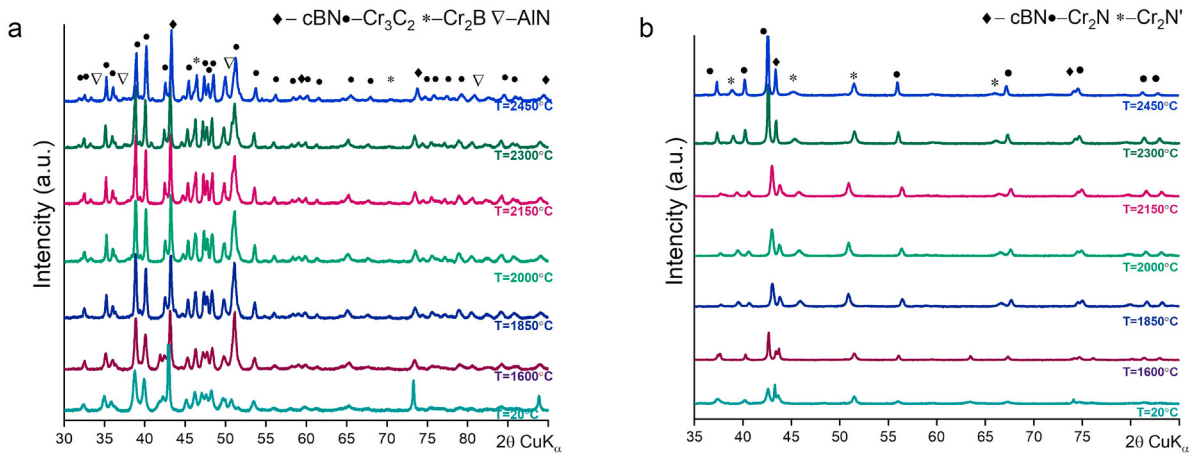

Figure 2. XRD patterns of the samples of cBN-Cr_3C_2-Al (a) and cBN-Cr_2N-Al (b) systems sintered at a pressure of 7.7 GPa for 45 s in the temperature range of 1600-2450°C and initial powder mixture - 20°C.

Phase composition remains unchanged as long as sintering temperature remains below 2150°C. At this temperature, chemical interactions between the components begin and the formation of CrB_2 and AlN is observed. In addition, some $C_{graphite}$ appears at the highest sintering temperature. It can be assumed that $C_{graphite}$ might be present even at lower temperatures (2150 - 2300°C), but its amount is insufficient for detection by XRD. The interactions occur according to the following reaction:

$$6BN + Cr_3C_2 + 6Al \rightarrow 3CrB_2 + 6AlN + 2C_{graphite}$$

XRD patterns of the samples of cBN-Cr_2N-Al system sintered at 7.7 GPa are shown in Figure 2b. Analysis of the initial Cr_2N powder after milling shows that it consists of two chromium nitride phases: CrN (Pm3m with lattice parameters a = 4.1759 Å) and Cr_2N (P-31m with lattice parameters a = 4.8260 Å, c = 4.5091 Å). Therefore, the initial powder mixture (T = 20°C in Figure 2b) consists of cBN, Cr_2N, CrN and Al (the latter is not identifiable with XRD). When applying pressure and temperature, interactions between cBN and chromium nitride were not observed. Thermobaric sintering have no impact on the phase composition of samples in cBN-Cr_2B-Al system, interactions between components of the mixture were not found.

3.2. Microstructure

Figure 3 shows typical SEM microstructures of our PcBN materials. The micrographs are secondary electron images revealing compositional contrast between different phases. The microstructure of all samples consists of approximately 60 vol.% of cBN grains which are visible as dark grey areas. The grains are uniformly surrounded by the binder phase. It is clearly visible that the cBN grain size is from 0.5 μm to 2 μm.

cBN–Cr_3C_2-Al system. At relatively low sintering temperatures (Figure 3a) the cBN phase has sharp grain boundaries, which confirms the absence of interaction between components. The light grey areas correspond to Cr_3C_2. When chemical interactions begin, the morphology of cBN grains changes to more a round shape (Figure 3d). Reaction products CrB_2 and AlN agglomerate at the interface boundaries.

cBN–Cr_2N-Al and cBN-CrB_2-Al systems. General view of microstructure does not change even at high sintering temperature. The cBN grains are uniformly surrounded by the binder phase and do not change the morphology.

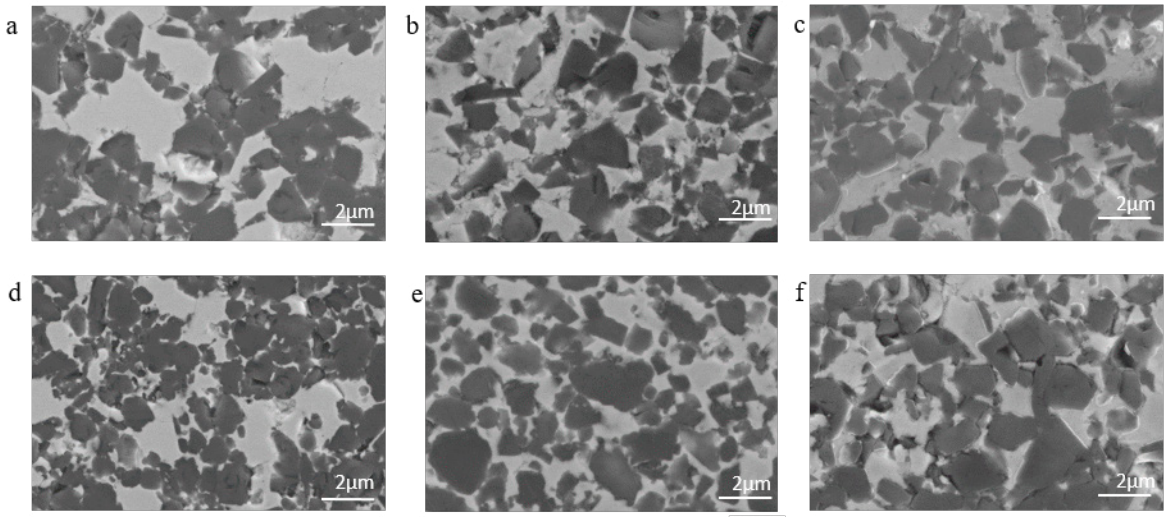

Figure 3. SEM of microstructures of the samples of cBN-Cr_3C_2-Al sintered at 1850°C (a) and 2300°C (d), cBN-Cr_2N-Al sintered at 1600°C (b) and 2450°C (e), cBN-CrB_2-Al sintered at 1850°C (c) and 2450°C (f) under a pressure of 7.7 GPa for 45 s.

3.3. Mechanical properties

Measurements of the green compact obtained under a pressure of 7.7 GPa but without heating show that its density is 25-30% lower than the full-dense body (Figure 4a). After heating to 1600°C the density reaches 90-97% of the theoretical value. Further increase of sintering temperature does not significantly affect the density.

Elastic moduli of the sintered samples of cBN-Cr_3C_2-Al system have a two-step change. The first stage is a sharp increase of Young's modulus from 450 GPa to 550 GPa in the temperature range of 1600 - 1850°C (Figure 4c). The second stage is observed when the chemical reaction between components takes place. The elastic modulus decreases

at 2150°C and increases again at higher sintering temperatures. This can be explained by the increment of the volume of reaction products. Young's modulus in the cBN–Cr_2N-Al system is not subject to temperature influence and remains at around 570 GPa throughout the whole series of experiments. The samples from cBN-CrB_2-Al system have the highest level of Young's modulus. Both systems have the same tendency for the growth of shear modulus with increase of the sintering temperature (Figure 4b).

For estimation of the predicted hardness of sintered composites a model of a simple mechanical mixture were applied. This model does not take into account the strength of the interphase boundaries and products of chemical interactions which may take place in the mixture. As a result of the calculations, it can be assumed that the predicted value of hardness is 30 GPa for cBN-Cr_3C_2-Al, 32 GPa for cBN-Cr_2N-Al and 33GPa for cBN-CrB_2-Al.

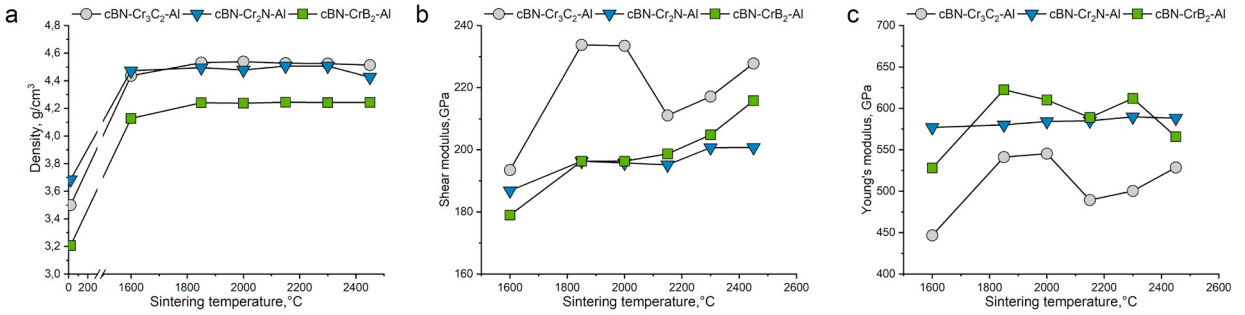

Figure 4. Density (a), Shear modulus (b) and Young's modulus (c) versus sintering temperature.

Comparing the experimental results with predictions, it can be assumed that at low sintering temperatures (1600°C) the interphase boundaries are still weak. The measured hardness of samples are lower than the predicted value. When the temperature increases up to 1850°C, the interphase boundaries attain sufficient strength, so that the hardness is comparable to the predicted value. So, the experimental hardness is higher than the predicted one and is in the range of 31 - 37 GPa depending on the system (Figure 5). The maximum hardness for the systems with carbide and nitride bonds is observed at 2000°C. Sintering at higher temperatures leads to reduction of the crystal defect density. As a consequence, recovery and potentially recrystallization is occuring and this leads to material softening. Increasing of the defectivnes of the structure promote the movement of dislocations in the material and this effect on the hardness. The highest and most stable value of fracture toughness observed for the cBN-Cr_3C_2-Al system is 5.5 MPa·$m^{1/2}$ (Figure 5b). A typical indentation imprint is shown in Figure 5c.

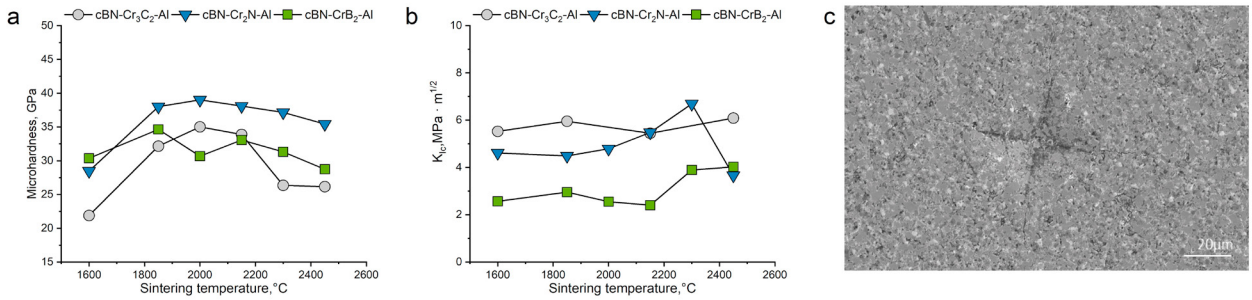

Figure 5. Hardness (a) and fracture toughness (b) versus sintering temperature; SEM image of indenter imprint in cBN-Cr_3C_2-Al system sintered at 2150°C (c).

3.4. Cutting performance

Figure 6 shows the tool wear development for the investigated systems during machining stainless steel AISI 316L at two cutting speed levels. General trends are clearly visible for all tested systems. Firstly, all samples sintered at 1600°C, with correspondingly lowest mechanical and physical properties, demonstrated the most intensive tool wear (650 - 900 µm at v_c = 500 m/min). Similar behavior is also observed for the samples sintered at 1850°C, even though they are more densified (Figure 4a). Secondary, the lowest values of tool wear (200 – 300 µm at v_c = 500 m/min) are observed for the samples sintered at temperature range 2000 - 2150°C, they have the highest level of mechanical properties and relative density around ~97%. Flank wear for samples sintered with Cr_3C_2 and Cr_2N binders at temperatures above 2000°C is not particularly effected by cutting speed. System cBN-CrB_2-Al has significantly accelerated tool wear at cutting speed of 500m/min (Figure 6c). Figure 7 depicts the light optical micrographs of the flank face of the work tools. It can be assumed that in machining of AISI 316L the prevailing wear mechanism is the diffusional and chemical as in the other cases when machining austenitic materials [19]. Optical images of the flank wear (Figure 7c, f) confirm, relative to the other investigated systems, more intensive material degradation.

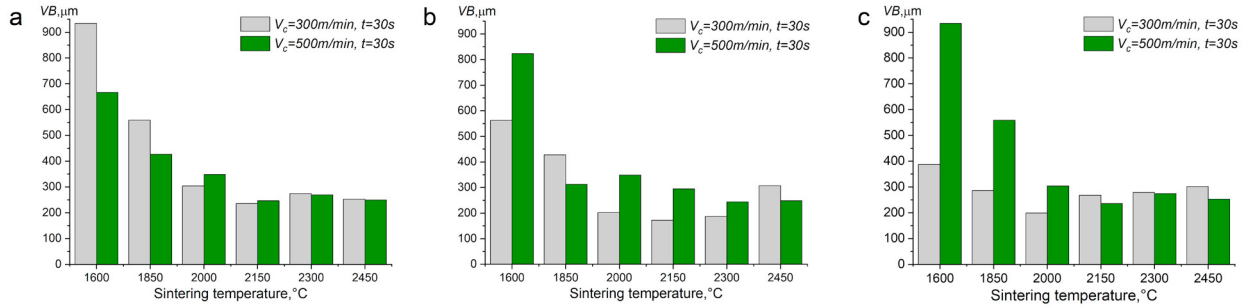

Figure 6 Tool wear development when machining 316L with samples from cBN-Cr_3C_2-Al system (a), cBN-Cr_2N-Al system (b) and cBN-CrB_2-Al system (c).

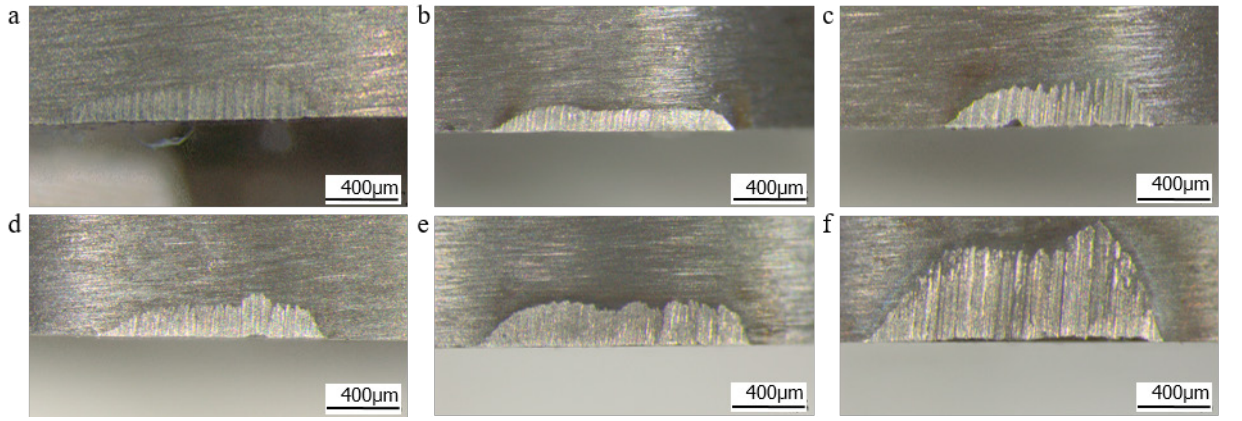

Figure 7 Optical images of cutting edge when machining AISI 316L with samples from cBN-Cr_3C_2-Al system v_c=300m/min (a), v_c =500m/min (d) cBN-Cr_2N-Al system v_c =300m/min (b), v_c =500m/min (e) and cBN-CrB_2-Al system v_c =300m/min (c), v_c =500m/min (f), all samples sintered at 2150°C.

When machining Vanadis 4E tool wear development is significantly higher in systems with CrN and CrB_2 binders, as compared to the system with Cr_3C_2 (Figure 8). As expected, tool wear in all systems is lower under lower cutting speed. Optical images of worn tool in system with CrN shown complete failure of the cutting tool after 600m of engagement length on Vanadis 4E (Figure 9 b,e). When analysing the results of the tool wear testing it can be concluded that the samples in cBN-Cr_3C_2-Al system at temperatures above 2000°C shows the lowest level of tool wear (Figure 9 a,d). Flank wear observed in cBN-CrB_2-Al system is slightly bigger while machining of Vanadis 4E

(Figure 9 c,f), in addition to the good results demonstrated during machining of AISI 316L. Since the microstructure of Vanadis 4E steel contains abrasive particles (MC carbides), it can be assumed that the dominant wear mechanism is abrasive wear [20] in combination with diffusional wear [21].

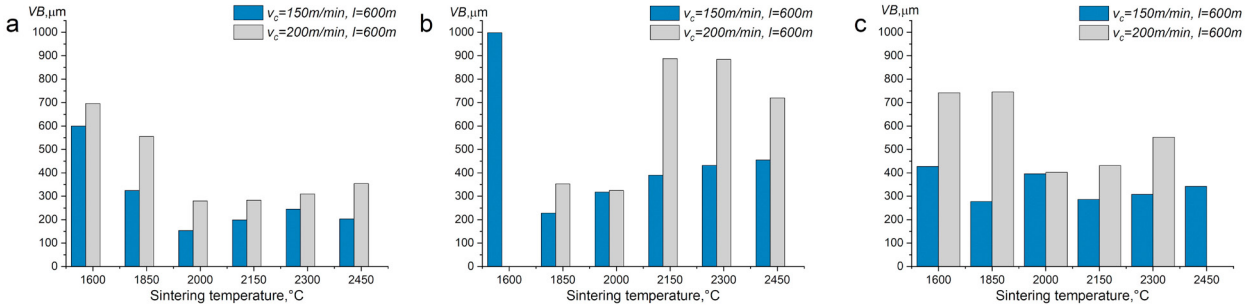

Figure 8 Tool wear development when machining Vanadis 4E with samples from cBN-Cr_3C_2-Al system (a), cBN-Cr_2N-Al system (b) and cBN-CrB_2-Al system (c).

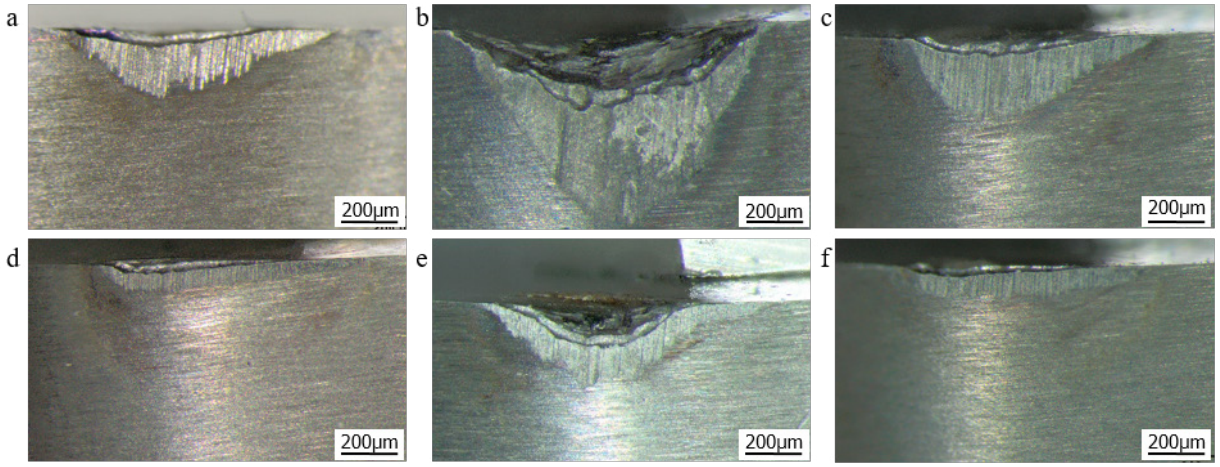

Figure 9 Optical images of cutting edge when machining Vanadis 4E with samples from cBN-Cr_3C_2-Al system v_c =200m/min (a), v_c =150m/min (d) cBN-Cr_2N-Al system v_c =200m/min (b), v_c =150m/min (e) and cBN-CrB_2-Al system v_c =200m/min (c), v_c =150m/min (f), all samples sintered at 2150°C.

It should be noted that despite the observed superior mechanical properties of the obtained PcBN materials in the designated systems their performance in machining operations of AISI 316L and Vanadis 4E workpiece materials was significantly less than the acceptable industrial standard. This is most likely related to the reduced chemical stability and higher diffusional wear of the binder systems compared to the commercial TiC or Ti(C,N) binders.

4. Conclusions

In this work, mechanical properties and cutting performance of cBN-based materials with new binders were investigated. It can be concluded that the optimal temperature range for sintering of superhard cBN-based materials with Cr_3C_2, Cr_2N and CrB_2 binders under a pressure of 7.7 GPa is 1800-2150°C. Interactions between components of the mixture occur in the cBN-Cr_3C_2-Al system. At sintering temperatures above 2150°C, CrB_2 and AlN are formed, which affects the cBN grain morphology and leads to degradation of the mechanical properties. HPHT sintering in the cBN-Cr_2N-Al and cBN-CrB_2-Al systems takes place without chemical interaction. The highest value of the hardness is observed for the composites with Cr_3C_2 and CrB_2 binders sintered at a temperature of 2000°C.

The highest tool wear resistance is demonstrated by the tools sintered at 2000 - 2150°C. During machining of AISI 316L this applies to all systems except cBN-CrB_2-Al, while for machining Vanadis 4E this applies only for tools in the cBN-Cr_3C_2-Al system.

Acknowledgments

This research was supported by European Union's Horizon 2020 Research and Innovation Programme under Flintstone2020 project (grant agreement No. 689279) and Visby Scholarship by the Swedish Institute (grant number 02757/2016). It is also a part of the Sustainable Production Initiative cooperation between Lund University and Chalmers University of Technology.

References

[1] Wentorf, R. H., DeVries, R. C., & Bundy, F. P. (1980). Sintered superhard materials. *Science*, 208(4446), 873-880.
[2] Eko, A., Fukunaga, O., & Ohtake, N. (2014). Morphology of cubic boron nitride crystals synthesized using (Fe, Co, Ni)–(Cr, Mo)–Al alloy solvents under pressure. *Diamond and Related Materials, 44*, 33-37.
[3] McKie, A., Winzer, J., Sigalas, I., Herrmann, M., Weiler, L., Rödel, J., & Can, N. (2011). Mechanical properties of cBN–Al composite materials. *Ceramics International, 37*(1), 1-8.
[4] Benko, E., Morgiel, J., & Czeppe, T. (1997). BN sintered with Al: Microstructure and hardness. *Ceramics international, 23*(1), 89-91.
[5] Lv, R., Liu, J., Li, Y., Li, S., Kou, Z., & He, D. (2008). High pressure sintering of cubic boron nitride compacts with Al and AlN. *Diamond and related materials, 17*(12), 2062-2066.
[6] Wang, P. F., Li, Z. H., & Zhu, Y. M. (2011). Fabrication of high thermal conductive Al–cBN ceramic sinters by high temperature high pressure method. *Solid State Sciences, 13*(5), 1041-1046.
[7] Morgiel, J., & Benko, E. (1995). Microstructure of boron nitride sintered with titanium. *Materials Letters, 25*(1-2), 49-52.
[8] Yazu, S., Kohno, Y., Sato, S., & Hara, A. (1980). New CBN/TiN Composite Sintered Under Ultra-High Pressure. *Modern Developments in Powder Metallurgy, 14*, 363-371.
[9] Klimczyk, P., Benko, E., Lawniczak-Jablonska, K., Piskorska, E., Heinonen, M., Ormaniec, A., ... & Urbanovich, V. S. (2004). Cubic boron nitride—Ti/TiN composites: hardness and phase equilibrium as function of temperature. *Journal of alloys and Compounds, 382*(1), 195-205.
[10] Angseryd, J., Elfwing, M., Olsson, E., & Andrén, H. O. (2009). Detailed microstructure of a cBN based cutting tool material. *International Journal of Refractory Metals and Hard Materials, 27*(2), 249-255.
[11] Rong, X. Z., Tsurumi, T., Fukunaga, O., & Yano, T. (2002). High-pressure sintering of cBN-TiN-Al composite for cutting tool application. *Diamond and Related Materials, 11*(2), 280-286.
[12] Harris, T. K., Brookes, E. J., & Taylor, C. J. (2004). The effect of temperature on the hardness of polycrystalline cubic boron nitride cutting tool materials. *International Journal of Refractory Metals and Hard Materials, 22*(2), 105-110.
[13] Chiou, S. Y., Ou, S. F., Jang, Y. G., & Ou, K. L. (2013). Research on CBN/TiC composites Part1: Effects of the cBN content and sintering process on the hardness and transverse rupture strength. *Ceramics International, 39*(6), 7205-7210.
[14] Zhang, L., Lin, F., Lv, Z., Xu, C., He, X., Wang, W., ... & Xia, L. (2015). cBN–Al–HfC composites: Sintering behaviors and mechanical properties under high pressure. *International Journal of Refractory Metals and Hard Materials, 50*, 221-226.
[15] Slipchenko K.V., Stratiichuk D.A., Petrusha I.A., Turkevich V.Z. (2017), Thermobaric sintering of cBN-Cr3C2 composite. *Rock destructive and metal cutting tools – technique and technology of their manufacturing and application*, *20*, 263-269.
[16] Costes, J. P., Guillet, Y., Poulachon, G., & Dessoly, M. (2007). Tool-life and wear mechanisms of CBN tools in machining of Inconel 718. *International Journal of Machine Tools and Manufacture, 47*(7-8), 1081-1087.
[17] Rice, R. W., Wu, C. C., & Boichelt, F. (1994). Hardness‐Grain‐Size Relations in Ceramics. *Journal of the American ceramic society, 77*(10), 2539-2553.
[18] Khvostantsev, L. G., & Slesarev, V. N. (2008). High-pressure apparatuses of a high volume for physical investigations. *Physics-Uspekhi, 178*(10), 1099-1104.
[19] Bushlya, V., Gutnichenko, O., Zhou, J., Avdovic, P., & Ståhl, J. E. (2013). Effects of cutting speed when turning age hardened Inconel 718 with PCBN tools of binderless and low-cBN grades. *Machining Science and Technology, 17*(4), 497-523.
[20] Poulachon, G., Bandyopadhyay, B. P., Jawahir, I. S., Pheulpin, S., & Seguin, E. (2004). Wear behavior of CBN tools while turning various hardened steels. *Wear, 256*(3), 302-310.
[21] Angseryd, J., Coronel, E., Elfwing, M., Olsson, E., & Andrén, H. O. (2009). The microstructure of the affected zone of a worn PCBN cutting tool characterised with SEM and TEM. *Wear, 267*(5), 1031-1040.